An Adaptive IEEE 802.15.4a TH-TDMA UWB Industrial Field Level Network

Farah Haroon, Kazi. M. Ahmed
Telecommunications Field of Study, Asian Institute of Technology, Thailand
Email: {Farah.Haroon, kahmed}@ait.ac.th

Abstract— **We introduce the deployment of IEEE 802.15.4a in industrial field level communication, which is unexplored so far. Impulse radio-time hopping ultra wide band (IR-TH UWB) physical layer is robust against dense multipath fading and interferences. However, we propose an adaption in medium access control (MAC) to meet the major constraints of reliability and timeliness. The self configuring MAC overcomes the difficulties and limitations of specified carrier sense multiple access/collision avoidance (CSMA/CA), slotted Aloha and guaranteed time slots (GTS) mechanisms. Addressable TH codes in fixed time slots of modified superframe structure are used to handle asynchronous alarm requests during ongoing synchronous transmissions. Traffic modeling is presented and we derive the expressions for accessing delays of both the synchronous and asynchronous data traffics. The realistic industrial non line of sight (NLOS) channel environment of IEEE 802.15.4a is employed and the respective power delay profile (PDP) and cumulative density function (CDF) of instantaneous signal to noise ratio (SNR) are found. Moreover, for large number of resolvable multipath components (MPCs), we also propose a reduced complexity adaptive SRake receiver, which efficiently recovers the weak IR-TH UWB signals in dense multipath propagation and strong noise. In addition, we evaluate the error performance of the proposed receiver architecture in comparison with conventional SRake and additive white Gaussian noise (AWGN) correlation receivers. Our simulation results show a significant performance improvement with very less number of SRake fingers.**

Index Terms— **Adaptive SRake receiver, field level industrial network, IEEE 802.15.4a, industrial NLOS environment, synchronous and asynchronous data.**

I. Introduction

An industrial network is characterized as a three level network. The lower most field level contains hardware, software and protocols for an interconnection of sensors and actuators with a master controller. It handles two types of data traffic: synchronous and asynchronous with both reliability and timeliness. The synchronous data is updated periodically and deals with the transfer of sensor and actuator states. Comparatively on the occurrence of alarms and emergency events, the low latency asynchronous data appears aperiodically and is served on high priority basis.

Among the most popular license free wireless technologies such as Bluetooth, ZigBee and IEEE 802.11, IEEE 802.15.4a impulse radio time hopping ultra wide band (IR-TH UWB) physical layer (PHY) has a strong potential to bear harsh and rugged industrial environment. The peculiar characteristics reduce intersymbol interference (ISI) and the inherent discontinuity mitigates the effects of large electromagnetic interventions. With small duty cycle and very fine pulse durations, it is recommended in dense multipath propagated industrial field level communication [1]. Independent time hopping (TH) codes of different data streams allow multiple access communication without catastrophic collisions. The resultant drop off in data rate is not so critical for small size data packets of field level, where the major constraint is meeting deadlines with correctness.

The wireless activities in industrial scenario were mostly directed towards the involvement of IEEE 802.11 and its alternatives. Prospects and significance of UWB in industrial applications were indicated in [2]- [4]. Deployment of IR-TH UWB in industrial adhoc networks was focused in [5] and [6], but the efforts were merely confined to a position based routing strategy. A packet aggregating medium access control (MAC) protocol for direct sequence spread spectrum (DSSS) UWB in field level network was suggested in [7]. Carrier sense multiple access/collision avoidance (CSMA/CA) was used as a channel access mechanism to reduce the large acquisition time (time required by the receiver to achieve bit synchronization with the transmitter) of the PHY.

However, the selected high data rate DSSS PHY is more suitable for visualization and monitoring services in upper levels of an industrial network [1]. CSMA/CA requires clear channel assessment (CCA) by energy detection (ED), which is challenging in UWB PHY having low power spectral density (PSD). Decorrelation and preamble detection carrier sensing are also much more complex. It was therefore declared in [8], that CSMA/CA is not appropriate for such ultra wide bandwidth signals and the use of other channel access mechanisms should be investigated.

IEEE 802.15.4a medium access control (MAC) relies on a superframe structure of 16 time slots. The first slot is always reserved for synchronization and transmission of control information through beacons. The remaining slots are occupied either by a contention access period (CAP) or a contention free period (CFP). Due to inherent restraints of CSMA/CA in UWB technology, use of slotted Aloha is also allowed in CAP [9]. But, both the channel access mechanisms for synchronous data transfer between single master and abundant of slave nodes suffer from

Manuscript received January 31, 2010; revised April 18, 2010; accepted May 11, 2010.

doi:10.4304/jcm.5.7.571-580

severe imperfections and render implementation complexities and very high acquisition times. For low latency applications, superframe structure provides a maximum of seven time division multiple access (TDMA) guaranteed time slots (GTS) in CFP. On request of slave nodes, they are reserved and allocated by the main master controller. But, due to the involvement of two way handshaking signals and insufficient availability, their provision is inapt for asynchronous data transfer.

Scattering and reflections with heavy metallic objects in industrial (non line of sight) NLOS surroundings generate plenty of resolvable multipath components (MPCs) and a dense power delay profile (PDP). In contrast to office and residential environments, it imposes serious complexity on optimum Rake receiver architectures. The first ray also does not carry the maximum amount of energy. Selective-Rake (SRake) utilizing the strongest MPCs is therefore preferable over all-Rake (ARake) and partial-Rake (PRake) receivers. SRake reception in IEEE 802.15.4a industrial NLOS channel model (CM8) was simulated in [10]. It indicated an obligation of hundreds of SRake fingers, but no solution to solve this problem is yet proposed.

Motivated by above considerations and constrictions, we bring in IEEE 802.15.4a in low data rate industrial field level networks. However, some relevant adaption is recommended to meet the deadlines of asynchronous requests. A modified superframe structure with addressable TH codes in TDMA based time slots is suggested. It overcomes the problems of traditional CSMA/CA in UWB technology and is capable of handling both the synchronous and asynchronous data. We propose a self configuring MAC protocol to transfer data without any CCA and ED. Expressions of the respective access delays are derived along with traffic modeling. Another substantial contribution of our work is the evaluation of error performance of IR-TH UWB in realistic IEEE 802.15.4a industrial non line of sight (NLOS) environment of channel model 8 (CM8). The respective channel cumulative distribution function (CDF) is found, which indicates the distribution of instantaneous signal to noise ratio (SNR) among very large number of resolvable MPCs. We include an adaptive noise cancellation principle of [11] to conventional SRake reception of IR-TH UWB. The proposed adaptive SRake architecture cancels the noise from weak UWB signals and improves SNR through an adaptive recursive least square (RLS) algorithm. It overcomes the complexity of [10] and shows a substantial performance improvement as compared to conventional SRake and AWGN correlation receivers.

The rest of the paper is organized as follows. Section II gives an overview of the system model with complete details of signal construction and industrial NLOS channel model 8. Section III covers the proposed adaption and modifications at the MAC layer. Traffic modeling and the derivation of access delays are also included. Proposed receiver architecture is specifically discussed in Section IV. Numerical and simulation results are presented in Section V. Section VI concludes the final remarks.

II. System Model

We deploy IEEE 802.15.4a in field level communication between master controller acting like a personal area network (PAN) coordinator and number of slave nodes. They are all connected in star topology in IEEE 802.15.4a industrial NLOS environment of CM8 as shown in Figure 1. All the nodes are fixed and consist of a transceiver which either acts as a transmitter or a receiver. An antenna array with a main lobe and a side lobe is utilized to obtain the primary and reference inputs at the proposed adaptive SRake receiver. Following [11], at the primary input, the main lobe is used to supply the distant transmitted signal corrupted by noise. Where as, the required correlated version of primary noise at the the reference input is acquired by its respective side lobe. Uncoded IR-TH

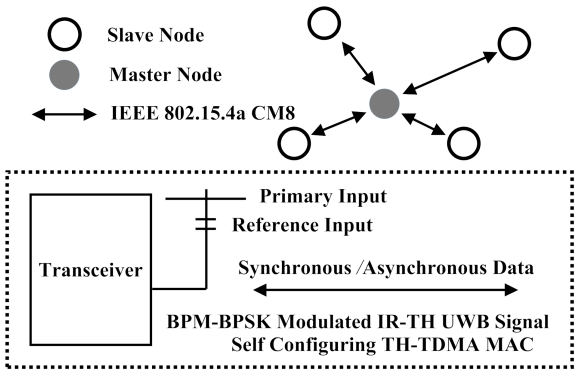

Figure 1. System Model

UWB, modulated using burst position modulation-binary phase shift keying (BPM-BPSK) is employed for both the synchronous and asynchronous data transfer at a center frequency of 7.987 GHz of channel 11 of high band plan [9]. In addition, a self configuring TH-TDMA MAC is proposed to reduce the accessing delay of asynchronous data classified into $q = 1, ..., Q$ priorities.

The detail of signal construction using addressable TH codes and IEEE 802.15.4a CM8 is as follows

A. Signal Construction using Addressable TH Codes

According to [9], data for coherent detection is modulated as a two bit symbol using BPM-BPSK. It generates a burst of duration T_{burst} using N_{cpb} consecutive pulses with each pulse occupying a small chip interval of T_c=2 ns. The burst can be present in any of the possible N_{hop} positions identified by independent TH codes, assigned to synchronous and each priority of asynchronous data. The code represents a sequence $[c_0^q, c_1^q, ..., c_{N_{hop-1}}^q]$ of integers defining respective burst locations in a data stream.

Although, specified pseudo-random TH codes with an unlimited number of independent sequences are very popular but due to the absence of any structure are also very difficult to address. Therefore, we assigned code to

each q^{th} priority class and synchronous data based on code construction 1 as mentioned in [12].

$$c_j^q = (q + j - 1)\ mod\ N_q \tag{1}$$

where N_q should be a prime number indicating the code length or period with a value taken between 0 and $N_{hop} - 1$.

The first data bit d_{jBPM}^{qc} encodes the position of the burst in either half of the symbol duration T_{BPM}, while the second data bit d_{jBPSK}^{qc} indicates its polarity. It generates a set of M=4 symbols using $m_b = 1, ..., M$ biorthogonal transmitted signals. For symbol energy E_s and $p_{tx}(t)$ as the first derivative Gaussian pulse, $s_{txm_b}^{qc}(t)$ is the m_b^{th} biorthogonal signal of q^{th} priority using c^{th} TH code given as below

$$s_{txm_b}^{qc}(t) = \sqrt{\frac{E_s}{N_{cpb}}} \sum_{j=-\infty}^{\infty} (1 - 2d_{jBPSK}^{qc})$$
$$\sum_{x=1}^{N_{cpb}} p_{tx}(t - c_j^q T_{burst} - xT_c - d_{jBPM}^{qc} T_{BPM}) \tag{2}$$

These M=4 signals can be completely constructed by $m = \frac{M}{2} = 2$ orthogonal signals and their inverses. If $d_{jBPSK}^{qc} = 0$ is kept in the above Eq.(2), $s_{txm}^{qc}(t)$ represents the m^{th} equivalent orthogonal signal expressed as

$$s_{txm}^{qc}(t) = \sqrt{\frac{E_s}{N_{cpb}}} \sum_{j=-\infty}^{\infty} \sum_{x=1}^{N_{cpb}} p_{tx}$$
$$(t - c_j^q T_{burst} - xT_c - d_{jBPM}^{qc} T_{BPM}) \tag{3}$$

In vector notation, these m signals can be shown by nonzero value in their m^{th} dimension as

$$\mathbf{s_{tx1}^{qc}} = (\sqrt{E_s}, 0) \tag{4}$$

$$\mathbf{s_{tx2}^{qc}} = (0, \sqrt{E_s}) \tag{5}$$

B. Industrial NLOS Channel Model 8

IEEE 802.15.4a industrial NLOS environment is available as CM8. The analysis is based on modified Saleh and Valenzuela (SV) model for indoor multipath propagation, which indicates that the grouping of objects in the surroundings leads to clustering of MPCs. Using a_{kl} and τ_{kl} as the gain and delay of k^{th} component of the l^{th} cluster and T_l as the arrival time of l^{th} cluster, the channel impulse response is given by

$$h(t) = \sum_{l=0}^{L-1} \sum_{k=0}^{K-1} a_{kl}\ \delta(t - T_l - \tau_{kl}) \tag{6}$$

It is evident from Eq.(6) that for a carrier less baseband IR-UWB, using pulse based transmitter and receiver, the channel response is represented as a real pass band system without considering the phase angles. It is in contrast to complex baseband technique which is used to express channel impulse responses of carrier modulated signals [13]. Their reception involve the generation of in phase and quadrature components. For amplitude variations, complex Gaussian best accounts over a small area, with an equivalent complex baseband Rayleigh distribution.

In the presence of large excess delays prevailing in NLOS industrial, the conventional distribution is no more valid for UWB bandwidth having fine time resolution of delay bins. Alternatively, Nakagami distribution with probability distribution function (PDF) shown in Eq.(7) has been suggested for small scale fading with a Lognormally distributed Nakagami m_l factor [14].

$$pdf(z) = \frac{2}{\Gamma(m_l)} (\frac{m_l}{\Omega})^{m_l}\ z^{2m_l - 1}\ exp\ (-\frac{m_l}{\Omega} z^2) \tag{7}$$

Where $\Gamma(m_l)$ is the gamma function and Ω is the mean square value of the amplitude.

In other environments, the PDP appears with Poisson distributed cluster and ray arrival times. In contrast, with a single cluster in industrial NLOS channel, it is expressed as

$$E\{|\ a_{kl}\ |^2\} = (1 - \chi\ exp\ (-\frac{\tau_{kl}}{\gamma_{rise}}))$$
$$exp\ (-\frac{\tau_{kl}}{\gamma_1})\ \frac{\gamma_1 + \gamma_{rise}}{\gamma_1} \frac{\Omega_1}{\gamma_1 + \gamma_{rise}(1 - \chi)} \tag{8}$$

Where χ represent the attenuation of first path. γ_{rise} and γ_1 respectively pertaining the rising and decaying time constants with Ω_1 as the integrated energy of first single cluster.

For the statistics of small scale fading and complete description of modified path loss functions, [15] can be consulted.

III. THE PROPOSED MAC FRAMEWORK

The data and management services under IEEE 802.15.4a are respectively provided through physical layer data-service access point (PD-SAP) and physical layer management entity-service access point (PLME-SAP).

Each node either master or slave acts as a transceiver present within the communication range of all the other nodes of the network. They remain in receiving state

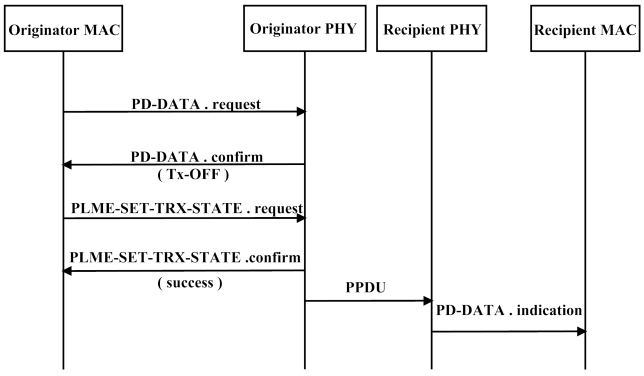

Figure 2. IEEE 802.15.4a message sequence for data transfer

with their transmitters disabled. However, if one wants to transmit, a PD-DATA.request primitive is assigned by a local MAC to its PHY as shown in Figure 2. In response, the local PHY delivers the PD-DATA.confirm primitive

to its MAC sublayer entity with a TX-OFF status. It leads MAC to issue a PLME-SET-TRX-STATE.request primitive to its PLME entity to disable the receiver (RX-OFF) and enable the transmitter (TX-ON). On successful change of state, physical layer service data unit (PSDU) is generated and transferred to the peer PHY. Finally the PD-DATA.indication primitive is generated by the receiving PHY to its MAC sublayer entity.

A. Data Traffic

The asynchronous and synchronous data in our system are modeled as

1) Asynchronous Data: It is classified into $q = 1, ..., Q$ classes with Q indicating the lowest asynchronous priority. The traffic arrival is modeled as a random Poisson (Markovian) process with exponentially independent and identically distributed inter arrival times. Each q^{th} class defines a separate queue with non preemptive Head On Line (HOL) discipline. They are served by one server, the master controller within fixed deterministic service time of T_s and modeled as Markovian/Deterministic/single server represented as M/D/1 traffic.

2) Synchronous Data: It has the lowest $Q+1$ priority and can be interrupted by any asynchronous request. Due to cyclic nature, it is updated periodically and is preferred to be buffered rather then being queued [16]. The old data present in the buffers is continuously replaced by the new ones in every cycle. To achieve data efficiency, periodic data does not need to be acknowledged as the receiver in case of occurrence of any error can wait for the correct data until the next cycle. The service time allowed is still equivalent to duration T_s. Although it occurs periodically but when executed with random asynchronous requests, is also treated as M/D/1 traffic.

B. Modified Superframe Structure

The MAC is based on a modified superframe structure and provides channel sensing functionality without incurring any extra complexity and overheads of ED and CCA. We assume the entire duration of the beacon enabled modified superframe structure of Figure 3 as an active period. All the slots are of fixed duration Ts with the first slot reserved for beacons from the master controller. The last 15 slots instead of being divided into CAP and CFP are all occupied by TDMA based contention free period. In normal operation, fixed scheduled synchronous

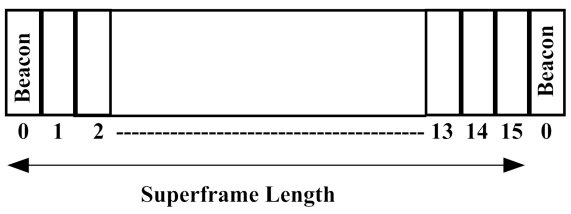

Figure 3. Modified contention free superframe architecture: Using TH codes asynchronous access is ensured in the next time slot without CCA and ED

data is transmitted on common TH code. On the occurrence of any alarm, the self configuring MAC delays the synchronous transmission and assigns the very next slot to the highest priority asynchronous request using a distinct TH code sequence. It avoids the use of standard GTS mechanism of [9] for low latency operations and hence overcomes the delay d_{GTS} expressed as a sum of

- d_{req}: time consumed in requesting a GTS from a slave node.
- d_{alloc}: on the availability and requirement, time spend in allocation of GTS by the master controller.
- d_{ack}: time wasted in number of acknowledgment transmissions.

Thus, the total delay d_{GTS} incurred in GTS management is averted, which is given as below

$$d_{GTS} = d_{req} + d_{alloc} + d_{ack} \tag{9}$$

C. Self Configuring TH-TDMA MAC

All the nodes are assumed within the communication range of each other having a complete knowledge of assigned TH codes of synchronous and asynchronous data. Although, the selected PHY efficiently supports multiple access communication based on distinct TH code sequences. But, for one to many or many to one directed master slave field level communication, single detection technique is more suitable. The operation starts from synchronous transmissions on common code sequence and continues as follows.

1) Identification: All the transmissions are completed within interval of time slot T_s. The header of the data packet holds the information about the used TH code. In addition, respective TH sequence is always interspersed in the end of data portion of every ongoing synchronous or asynchronous transmission. It provides channel sensing functionality and priority identification by all the receiving nodes without any ED and CCA.

2) Arrival: On the occurrence of alarm, the corresponding node acquires the transmitting state and signals the arrival of asynchronous request during the interspersed coded portion of the data packet. It first uses the TH sequence of the ongoing transmission which corrupts the embedded common code and indicates an arrival. Later, the alarm generating node employs respective self TH code which is registered in non preemptive HOL queue at all the receiving nodes. The transmission of cyclic data is postponed from the next scheduled node for one time slot and the alarm generating node transmits the data mixed with its code sequence in the forth coming slot.

3) Self Organization: If the synchronous processing has been resumed, the appearance of second asynchronous request is dealt as previously. Otherwise, on the basis of registered TH sequences, prioritized self configuring transmitting decisions at each node are taken and the respective alarms are sequentially processed. However, every new asynchronous request delays the synchronous transmission by one time slot.

D. Formulation of Delay

Requests of same priority generated from all nodes, form a separate queue with its respective arrival rate λ_q and service rate μ_q. Due to TDMA, mean service time of class q, $\overline{T}_q$ is constant and equals to slot duration T_s. It relates with μ_q and offered Poison traffic A_q as

$$\mu_q = \frac{1}{\overline{T}_q}, \ for \ \forall \ q = 1, ..., Q \tag{10}$$

$$Aq = \lambda_q \overline{T}_q \tag{11}$$

Thus the total asynchronous traffic offered to cyclic processing is given by

$$A_{asy} = \sum_{q=1}^{Q} A_q \tag{12}$$

The corresponding accessing delays of asynchronous and synchronous data on the basis of the proposed MAC are analyzed and formulated as below

1) Delay in Accessing of Asynchronous Data: On behalf of [17], the delay faced by an arbitrary asynchronous request of priority 'n' in being served is the sum of three factors

w_c = delay due to current ongoing transmission.
w_b = delay due to equal and higher priority requests that arrive before 'n'.
w_a = delay due to higher priority requests that arrive after 'n'.

a) Delay due to current transmission: This type of delay is always equal to mean residual service time of continuing request and can be determined using mean value analysis [18].
In our case, the slot assignment for an asynchronous alarm is either delayed due to ongoing synchronous or asynchronous transmission. The sum of the probabilities of being in either of two states would be 1 and the residual time by using mean value analysis can be written as

$$w_c = \overline{T}_{res} = p_{syn}\overline{T}_{syn} + p_{asy}\overline{T}_{asy} \tag{13}$$

The probability of occurrence of asynchronous data p_{asy} actually represents the total offered asynchronous traffic A_{asy}. The average time values of both the synchronous and asynchronous data respectively represented as $\overline{T}_{syn}$ and $\overline{T}_{asy}$ are equivalent to slot duration T_s. Thus, w_c is given by

$$w_c = (1 - \sum_{q=1}^{Q} A_q)T_s + \sum_{q=1}^{Q} A_q T_s = T_s \tag{14}$$

b) Delay due to equal and higher priority requests that arrive before 'n': Considering the arrival of an arbitrary asynchronous request with priority 'n', before which the requests of equal and higher priorities are already present. Let $\overline{N}_{qb}$ be the expected number of requests from individual priority q when $q \leq n$, then each of such request will arrive with an arrival rate λ_q and require to be serviced. Its value using Little equation for a period w_q (time up to the occurrence of q) is given as

$$\overline{N}_{qb} = \lambda_q w_q \tag{15}$$

Thus, the waiting time due to requests from all such classes equals to

$$w_b = \sum_{q=1}^{n} \overline{N}_{qb} \ \overline{T}_q = \sum_{q=1}^{n} A_q w_q \tag{16}$$

c) Delay due to higher priority requests that arrive after 'n': Equal priority requests are not considered due to HOL discipline with in one priority class. Let $\overline{N}_{qa}$ be the expected number of requests from individual priority q, when $q < n$ with a duration that can extend up to w_{asy}. The respective waiting time is expressed as

$$w_a = \sum_{q=1}^{n-1} \overline{N}_{qa} \ \overline{T}_q = \sum_{q=1}^{n-1} A_q w_{asy} \tag{17}$$

Now the overall delay in processing of asynchronous data of n^{th} priority will be given by

$$w_{asy} = T_s + \sum_{q=1}^{n} A_q w_q + \sum_{q=1}^{n-1} A_q w_{asy} \tag{18}$$

As w_{asy} is the delay in accessing of n^{th} asynchronous request represented by w_n, then the above equation is simplified as

$$w_{asy} = \frac{T_s + \sum_{q=1}^{n-1} A_q w_q}{1 - \sum_{q=1}^{n} A_q}, \quad n = 1, ..., Q \tag{19}$$

E. Delay in Processing of Synchronous Data

The delay in synchronous data due to the arrival of n^{th} asynchronous request is the sum of the accessing delay w_{asy} and the mean service time of n^{th} arrival.

$$w_{syn} = w_{asyn} + T_s \tag{20}$$

where T_s is the time spent during the transmission of n^{th} asynchronous request. The resultant delay in synchronous processing is therefore given by

$$w_{syn} = \frac{T_s(2 - \sum_{q=1}^{n} A_q) + \sum_{q=1}^{n-1} A_q w_q}{1 - \sum_{q=1}^{n} A_q}, \ n = 1, ..., Q \tag{21}$$

IV. An Adaptive SRake Receiver

In frequency selective IEEE 802.15.4a UWB channel, under the slow fading assumption the gain a_k and the delay τ_k of the k^{th} MPC are taken constant over a symbol duration. If all such K paths exhibit negligible correlations, then $\{a_k\}_{k=0}^{K-1}$ are treated statistically independent random variables with their PDF presenting Nakagami distribution. In the presence of AWGN, which is assumed as independent of fading amplitudes a_k having N_0 (W/Hz) as single sided power spectral density, the instantaneous SNR of k^{th} path per symbol having E_s energy is given by

$$\gamma_k = (a_k^2 E_s)/N_0 \tag{22}$$

and the respective total received instantaneous SNR would be

$$\gamma = \sum_{k=0}^{K-1} \gamma_k \tag{23}$$

In our system, a set of M=4 biorthogonal signals of uncoded IEEE 802.15.4a IR-TH UWB is transmitted through an industrial NLOS environment of CM8 in the presence of AWGN as shown in Figure 4. Addition

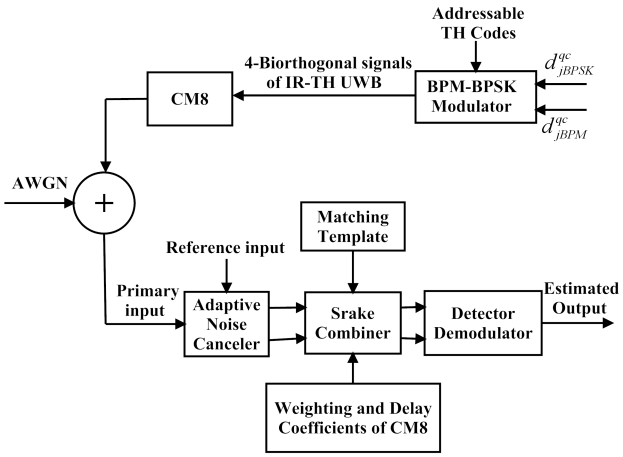

Figure 4. A transceiver system with proposed receiver architecture

of noise engulf the dense multipath propagated weak UWB signals which results in an increased complexity of SRake reception. A receiver architecture is proposed that includes an adaptive noise canceler (ANC) with primary and reference inputs, SRake combiner and a detector followed by a demodulator. Instead of utilizing M=4 biorthogonal signals, the SRake combiner is comprised of two independent Rake units for the respective $\frac{M}{2}$ orthogonal signals which reduces the required Rake units by half [19]. In addition to weighting and delay coefficients, the matching template also rely on the impulse response of CM8. The detector estimates one of $\frac{M}{2}$ signals based on highest magnitude of correlation sum. The sign of correlation sum finally decides one of M biorthogonal signals.

The sections of the proposed receiver architecture of Figure 5 utilizing K_s strongest MPCs include

A. RLS Adaptive Noise Canceler

For m^{th} transmitted signal, the respective mutually and statistically independent and identically distributed (iid) AWGN random variable has zero mean and variance given by

$$\sigma_m^2 = \frac{N_o}{2}, \quad m = 1, ..., \frac{M}{2} \tag{24}$$

While neglecting the antenna effects and assuming $h(t)$ as the impulse response of CM8, the received signal at the primary input of ANC is represented as $s_{rxm}^{qc}(t)$. If $*$ indicates the convolution operation and $n_{pm}(t)$ as the

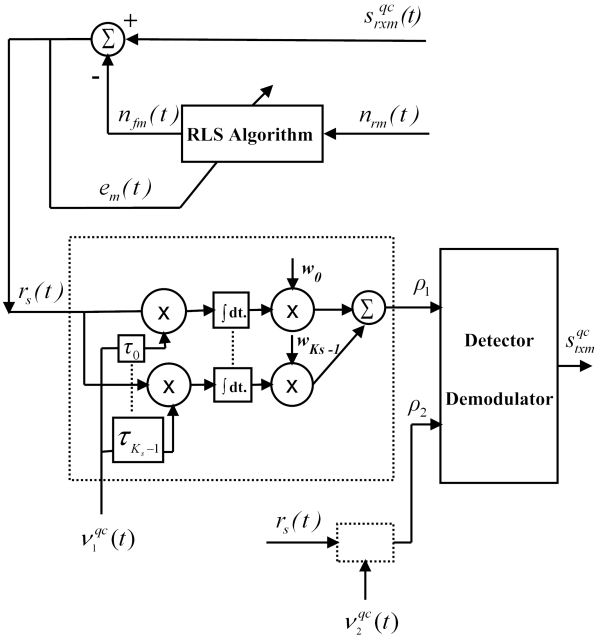

Figure 5. Adaptive SRake receiver operating in IEEE 802.15.4a industrial NLOS CM8, using an equivalent $\frac{M}{2}$ orthogonal signals instead of M biorthogonal signals

primary noise added into the m^{th} signal, $s_{rxm}^{qc}(t)$ is given by

$$s_{rxm}^{qc}(t) = s_{txm}^{qc}(t) * h(t) + n_{pm}(t) \tag{25}$$

Using i as time index the above equation is written as

$$s_{rxm}^{qc}(i) = s_{txm}^{qc}(i) * h(i) + n_{pm}(i) \tag{26}$$

where $s_{txm}^{qc}(i) * h(i)$ designates our desired response $d_m(i)$ free from noise $n_{pm}(i)$. The noise $n_{rm}(i)$, a correlated version of primary noise appears at the reference input. It was applied at the first tap input of the M_w order tap weight vector. After being adaptively filtered as $n_{fm}(i)$, it was subtracted from the primary input to produce an error signal $e_m(i)$ at the output of an ANC.

$$e_m(i) = s_{rxm}^{qc}(i) - n_{fm}(i) \tag{27}$$

It minimizes the squared error via RLS algorithm of [20]. The filtered noise $n_{fm}(i)$ was adjusted such that the noise power present in the primary input was reduced keeping the signal power unchanged. Thus, for the length of the observed data y, our objective function $\varepsilon_m(y)$ is given by

$$\varepsilon_m(y) = \sum_{i=1}^{y} \beta_m(y,i) \mid e_m(i) \mid^2 \tag{28}$$

To minimize the objective function, the algorithm on the basis of initial known conditions and feed back samples recursively updates the old estimates of tap weight vector $\mathbf{w_m}(y)$.

During the observation interval $1 \leq i \leq y$, the forgetting factor $0 \leq \beta_m(y,i) \leq 1$ of Eq.(29) is introduced to exponentially ignore the effect of past data.

$$\beta_m(y,i) = \alpha_m^{y-i} \tag{29}$$

where α_m is a positive constant close to, or equal to 1. The tap weight vector modifies the error signal according to

$$\mathbf{e_m}(i) = \mathbf{s^{qc}_{rxm}}(i) - \mathbf{w_m}^H(y)\mathbf{n_{rm}}(i) \quad (30)$$

when $\mathbf{s^{qc}_{rxm}}(i)$ indicates the time indexed sampled values of the received signal and $\mathbf{w_m}^H(y)$ at $(t = y)$ represents the conjugate transpose of $\mathbf{w_m}(y)$.
Both the tap weight vector $\mathbf{w_m}(y)$ and the time indexed reference noise vector $\mathbf{n_{rm}}(i)$ are expressed as

$$\mathbf{w_m}(y) = [w_{m0}(y), w_{m1}(y), ..., w_{m(M_w-1)}(y)]^T \quad (31)$$

$$\mathbf{n_{rm}}(i) = [n_{rm}(i), n_{rm}(i-1), ..., n_{rm}(i-M_w+1)]^T \quad (32)$$

The optimum value of the tap weight vector, at which our objective function acquires the minimum, is represented as $\hat{\mathbf{w}}_\mathbf{m}(y)$. According to [20], it is the product of the inverse of $\mathbf{\Phi_m}(y)$ and $\theta_\mathbf{m}(y)$ written as

$$\hat{\mathbf{w}}_\mathbf{m}(y) = \mathbf{\Phi^{-1}_m}(y)\theta_\mathbf{m}(y) \quad (33)$$

where $\mathbf{\Phi^{-1}_m}(y)$ is the M_w by M_w time averaged correlation matrix of tap inputs given by

$$\mathbf{\Phi^{-1}_m}(y) = \sum_{i=1}^{y} \alpha_m^{y-i}\mathbf{n_{rm}}(i)\mathbf{n_{rm}}^H(i) \quad (34)$$

and $\theta_\mathbf{m}(y)$ of m^{th} signal is the M_w by 1 time averaged cross correlation vector between the tap inputs and the complex conjugation of desired response $\mathbf{d_m}(i)$ indicated as

$$\theta_\mathbf{m}(y) = \sum_{i=1}^{y} \alpha_m^{y-i}\mathbf{n_{rm}}(i)\mathbf{d_m}^*(i) \quad (35)$$

The received signal after being adaptively filtered at the output of ANC is represented as $r_s(t)$. It was applied to both the Rake units, where the resultant increased SNR was effectively utilized to reduce the required number of fingers.

B. SRake Combiner

The branch statistic of SRake Combiner was found by generating an impulse response of CM8 according to [21]. 100 realizations of channel impulse response $h(t)$ were produced at each sampling interval T_s whose average gave the channel vector $\mathbf{h}$ with the corresponding time index vector $\mathbf{t}$.
Representing the strength of all the received K MPCs, $\mathbf{h}$ was then sorted for K_s strongest MPCs in $\mathbf{h_s}$ with time index $\tau_\mathbf{s}$ as

$$\mathbf{h_s} = [h_0(\tau_0), h_1(\tau_1), ..., h_{(K_s-1)}(\tau_{K_s-1})]^T \quad (36)$$

$$\tau_\mathbf{s} = [\tau_0, \tau_1, ..., \tau_{(K_s-1)}]^T \quad (37)$$

The above two vectors respectively represent the branch weighting coefficients $\mathbf{w_s}$ and delay elements of SRake combiner. A set of K_s fingers (branches) in each m^{th} Rake unit is indicated by a dashed box in Figure 5.

The locally generated matching template $\nu_m^{qc}(t)$ after neglecting the antenna effects was selected for one complete symbol duration. For m^{th} signal using c^{th} TH code assigned to q^{th} priority class, we selected it as

$$\nu_m^{qc}(t) = s_{txm}^{qc}(t) * h(t) \quad (38)$$

The received signal in each branch was correlated with the matching template delayed by τ_s and weighted by w_s. The sum of all the branch outputs corresponds to a maximal ratio combiner (MRC), which was treated as a decision metric ρ_m given by

$$\rho_m = \sum_{s=0}^{K_s-1} w_s.C_m(r_s(t), \nu_m^{qc}(t-\tau_s)) \quad (39)$$

where $C_m(a, b)$ represents the correlation between a and b entities.
Both of these ρ_m values for the two orthogonal signals fed into a detector/demodulator for final estimation of the transmitted symbol.

C. Detector

Assuming perfectly synchronized transmitter and receiver, the signal detection was analyzed and simulated as a single q^{th} data stream using c^{th} TH code. The estimated signal $\tilde{s}_{txm}^{qc}(t)$ was based on maximum likelihood (ML) detection expressed as

$$\tilde{s}_{txm}^{qc}(t) = \arg\max_m \mid \rho_m \mid \quad (40)$$

Later, either of $s_{txm}^{qc}(t)$ or -$s_{txm}^{qc}(t)$ was selected on behalf of the sign of the weighted largest correlation sum. Thus employing an equivalent orthogonal set, one of M signal was selected using $\frac{M}{2}$ cross correlators. The corresponding estimated symbol was finally provided by a demodulator.

V. Numerical and Simulation Results

A. Delay Evaluation

The accessing delays of $n = 1$ to Q asynchronous priorities were found numerically using Eq.(19). These delays are respectively shown in Figure 6 for slot duration $T_s = 0.01$ s, $Q = 5$, $w_q = 100$ hrs and the arrival vector $\lambda_\mathbf{q}$ of Eq.(41) in requests/hr.

$$\lambda_\mathbf{q} = [0.001, 0.005, 0.001, 0.002, 0.015]^T \quad (41)$$

It can be observed that an arbitrary n^{th} request belonging to q = 1 highest priority faces a delay equivalent to slot duration T_s. Where as, the delays faced by other priorities also depend on their arrival rates and time of occurrences.

Delay due to equal and higher priority requests that appear before n^{th} customer directly affects w_{asy} and depends on the period w_q. Using the same arrival vector, the asynchronous access delays for $n = 1$ to Q priority requests for the period w_q ranging from 100 to 600 hrs were found numerically and plotted in Figure 7. It can be observed that delay faced by the highest priority test customer is independent of the variations of w_q and is

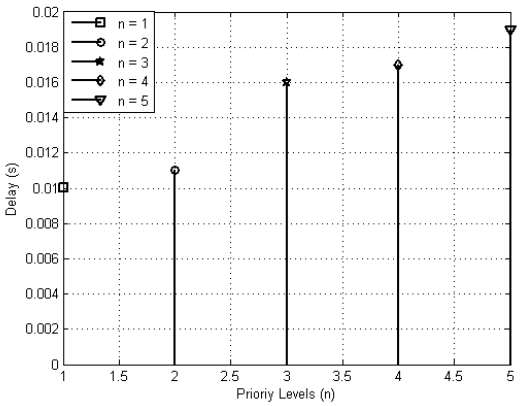

Figure 6. Accessing delays of $n = 1, ..., Q$ priority asynchronous data at w_q = 100 hrs

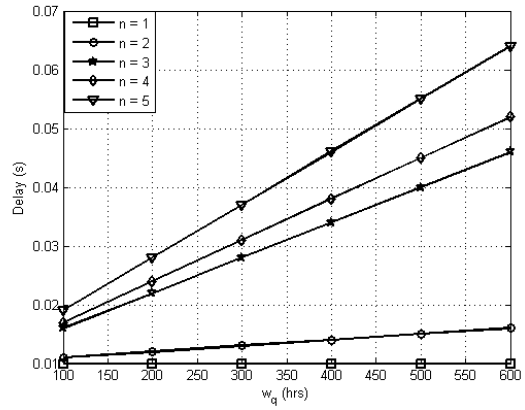

Figure 7. Accessing delays of $n = 1, ..., Q$ priority asynchronous requests as a function of w_q

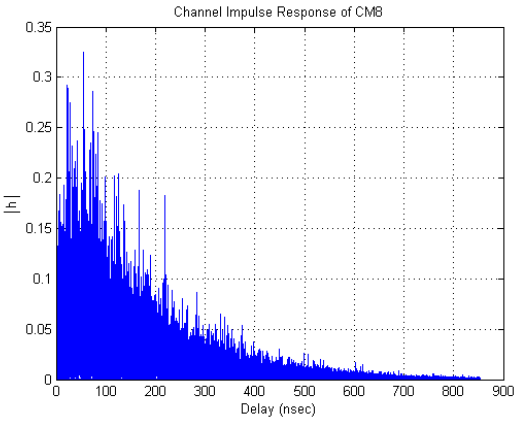

Figure 8. Channel impulse response: Average over 100 CM8 channels

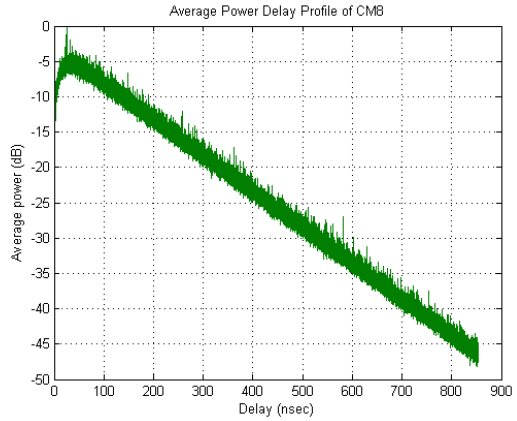

Figure 9. Power delay profile of CM8

always equivalent to slot duration T_s. However, at small arrival rates, effect of w_q dominates especially for $n = 3$ to 5 lower priorities .

B. Characteristics of Industrial NLOS Channel

Simulations were carried out in IEEE 802.15.4a industrial NLOS environment of CM8 at a center frequency $f_c = 7.987$ GHz of channel 11 of high band plan. Using a sampling frequency of $f_s = 50$ GHz, the channel impulse response and average PDP were generated as shown in Figure 8 and Figure 9. Both of them confirm the previous discussion and clearly indicate that the first arriving component in industrial NLOS does not exhibit the highest magnitude.

The CDFs of instantaneous received SNR from 20 and 100 strongest MPCs in CM8 were acquired for 1000 channel realizations in Figure 10. For it, discrete probability distribution functions (PDFs) were obtained from respective histograms for 0 dBs transmitted symbol energy. As a result, a gain of only 5 dBs is achieved when strongest MPCs are increased from 20 to 100 in channel environment following Nakagami probability distribution. It suggests an obligation of large number of Rake fingers required to attain an appreciable increase in energy collection in dense multipath propagated industrial NLOS environment.

C. Performance of Adaptive Noise Canceler

For simulation purpose instead of obtaining the primary and reference signals from an antenna array, 1000 random samples of primary noise $n_{pm}(i)$ were generated at ($i = 1$ to 100) time instants. At each i^{th} time instant they were passed through a 32 order low pass filter (LPF) to obtain the respective correlated reference noise samples of $n_{rm}(i)$. In response, a correlation strength $\varphi_m(i)$ ranging from -0.08 to +0.07 was obtained between the two types of noise samples as depicted in Figure 11.

Both of these noise samples were fed into an ANC. For the simulation of RLS algorithm in $M_w = 32$ order tap weight vector, Identity matrix $\mathbf{I}$ was selected as $\mathbf{\Phi_m}(y)$ of Eq.(34). The tap weight vector $\mathbf{w_m}(y)$ was initialized using all zeros vector with the exponential weighting factor $\alpha_m = 1$. To keep the recursions in progress and for the initial setting of the correlation matrix, $\mathbf{\Phi_m}(y)$ was multiplied with a small positive value $\delta_m = 0.1$.

The impulse response of ANC is adapted via RLS algorithm to remove the noise traces from the primary

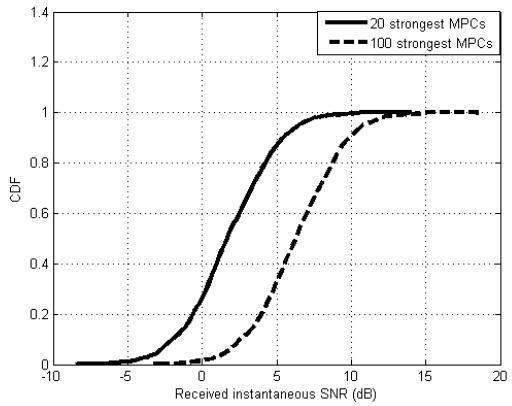

Figure 10. The CDF of received instantaneous SNR obtained from 20 and 100 strongest MPCs using 1000 channel realizations of CM8. At E_s = 0 dB and N_0= 1 W/Hz

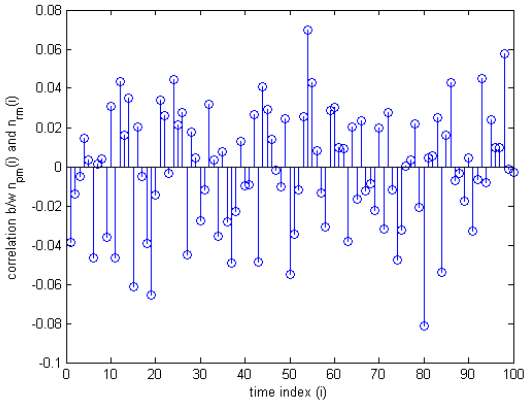

Figure 11. Correlation strength $\varphi_m(i)$ between primary and reference noise applied to an ANC at (t=i) time instants

signal. The obtained correlation strength between the desired response $d_m(i)$ and the output $r_s(i)$ varies between 0.65 to 0.9 as evidenced in Figure 12. It can be seen that even for $\phi_m(i)$ of less than 0.01, a correlation strength of greater then 0.6 between the desired response and the output of ANC is received.

D. BER Performance

According to [9], the values for channel 11 for f_c the center frequency, R_b the bit rate, T_c the chip duration, N_{cpb} the number of chips per burst, N_c the number of chips per symbol and N_{hop} the number of hops available per symbol are shown in Table I.

TABLE I.
PARAMETERS FOR CHANNEL 11

f_c(GHz)	R_b(Mb/s)	T_c(ns)	N_{cpb}	N_c	N_{hop}
7.987	0.85	2	16	256	8

Assuming synchronized transmitter and receiver and using the above mentioned parameters, the error performance of uncoded BPM-BPSK modulated IR-TH UWB

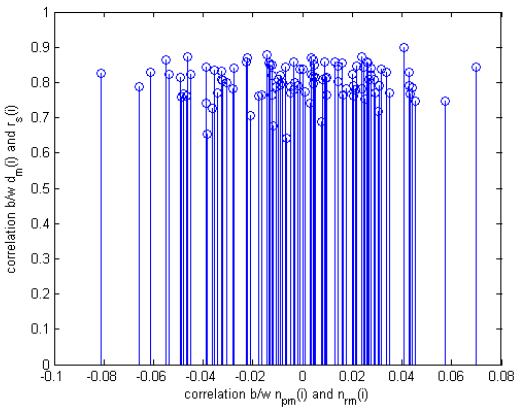

Figure 12. Correlation strength between desired response $d_m(i)$ and the output of ANC $r_s(i)$ due to applied $\phi_m(i)$

M biorthogonal signals was found in IEEE 802.15.4a industrial NLOS environment of CM8 in the presence of AWGN. Both the conventional SRake and adaptive SRake receivers employ 20 fingers in each Rake unit. The results are then compared in Figure 13 with those acquired via an AWGN correlation receiver. A significant performance improvement is achieved with an adaptive SRake which provides a gain of approximately 33 dBs and 5 dBs respectively with the conventional SRake and AWGN correlation receivers. It is therefore suggested, that instead of using hundreds of Rake fingers, an addition of an ANC drastically improves the error performance of conventional SRake in dense multipath propagated environment.

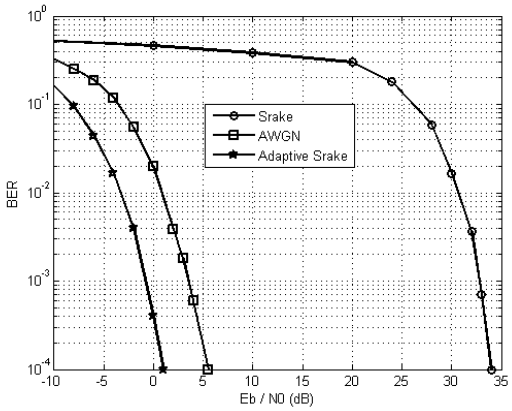

Figure 13. BER vs SNR of BPM-BPSK modulated uncoded IEEE 802.15.4a IR-TH UWB M-biorthogonal signals. SRake and adaptive SRake reception with 20 fingers: Average over 100 CM8 channel in the presence of AWGN in comparison over AWGN

VI. CONCLUSION

With an increasing demand of wireless technologies, our work serves as a first step toward deployment of IEEE 802.15.4a IR-TH UWB in dense multipath propagated noisy industrial environment. However, some adaption

was proposed to ensure required reliability and timeliness constraints of field level networks. The delay analysis indicates, that the proposed TH-TDMA MAC provides an urgent accessibility of asynchronous data during on going synchronous transmissions. It not only overcomes the delay of GTS management, but also avoids the use of CSMA/CA and slotted Aloha in UWB PHY. The channel characteristics were simulated and discussed. The proposed adaptive SRake architecture received the weak BPM-BPSK modulated IR-TH UWB biorthogonal signals with much decreased intricacy. The error performance depicts an appreciable improvement as compared to conventional SRake and AWGN receivers. As a direction for further research, the presented work should focus toward the ranging capability of the selected PHY and include mobility. Increase in the communication range based on multihop UWB networks and packet level simulations are another likely avenues for future research.

ACKNOWLEDGMENT

The first author expresses her gratitude to Higher Education Commission (HEC) of Pakistan, for providing scholarship opportunity and constant support for research funding.

REFERENCES

[1] X. Carcelle, T. Dang and C. Devic, "Industrial Wireless Technologies: Applications for the electrical utilities," *in Proc. IEEE International Conference on Industrial Informatics*, Aug. 2006, pp. 108–113.

[2] G. P. Hancke and B. Allen, "Ultrawideband as an Industrial Wireless Solution," *Pervasive Computing, IEEE Com Soc*, 2006, no. 4, pp. 78-85.

[3] D. Pellegrini, D. Miorandi, S. Vitturi and A. Zanella, "On the Use of Wireless Networks at Low Level of Factory Automation Systems," *IEEE Transactions on Industrial Informatics*, May 2006, vol. 2, no. 2, pp. 129– 143.

[4] G. Scheible, D. Dzung, J. Endresen and J. E. Frey, "Unplugged but connected - Design and Implementation of a Truly Wireless Real-Time Sensor/Actuator Interface," *IEEE Industrial Electronics Magazine*, 2007, vol. 1, no. 2, pp. 25–34.

[5] W. Zeng, H. Wang H. Yu and A. Xu,"The Research and Application of UWB Based Industrial Network," *in Proc. Ultrawideband and Ultrashort Impulse Signals, The Third International Conference*, Sept. 2006, pp. 153–155.

[6] W. Zeng, H. Wang H. Yu and A. Xu,"The Research of UWB Ad-Hoc Industrial Network," *in Proc. Communications and Networking in China, (ChinaCom)*, 25-27 Oct. 2006, pp. 1–4.

[7] J. Wang, W. Chen, H. Wang, and A. Xu, "Optimization on Delay and Slot Utilization for Fieldbus Control System Based on UWB," *in Proc. IEEE Conference on Industrial Electronics and Applications, ICIEA 2007*, May. 2007, pp. 1329-1333.

[8] A. Gupta and P. Mohapatra, "A survey on ultra wide band medium access control schemes," *Computer Networks 51, 2967-2993; available online at www.sciencedirect.com; Elesvier*, 2007.

[9] IEEE 802.15.4a-2007,"Part 15.4: Wireless Medium Access Control (MAC) and Physical Layer (PHY) Specifications for Low-Rate Wireless Personal Area Networks (WPANs); Amendment 1: Add Alternate PHYs," Mar. 2007.

[10] H. Gong, H. Nie and Z. Chen, "Performance Comparisons of UWB Selective Rake and Transmitted Reference Receivers under IEEE802.15.4a Industrial Environments," *in Proc. IEEE Wireless and Microwave Technology Conference (WAMICON)*, pp. 1–5, 2006.

[11] B. Widrow, J. R. Glover, J. M. McCool, J. Kaunitz, C. R. Williams, E. Dong and R. C. Goodlin, "Adaptive Noise Cancelling: Principles and Applications," *Proceedings of the IEEE*, vol. 63, no. 12, Dec. 1975.

[12] I. M. S. Iacobucci and D. M. Benedetto, "Multiple access design for impulse radio communication systems," *in Proc. IEEE Communications Conference, ICC '02*, vol. 2, pp. 817–820, 2002.

[13] S. G. Glisic and P. A. Leppanen, *Wireless Communications:TDMA vs CDMA*, Kluwer Academic Publishers, 1997.

[14] J. Karedal, S. Wyne, P. Almers, F. Tufvesson and A. F. Molisch, "A measurement Based Statistical Model for Industrial Ultra Wideband Channels," *IEEE Transactions on Wireless Communication*, vol. 6, no. 8, 2007.

[15] A. F. Molisch, K. Balakrishnan, D. Cassioli, C. C. Chong, S. Emami, J. Karedal, A. Fort, B. Kanan, J. Kunisch, H. G. Schantz, K. Siwiak and M. Z. Win, "A Comprehensive Standardized Model for Ultrawideband Propagation Channels," *IEEE Transactions on Antenna and Propagation*, vol. 54, no. 11 Part 1, pp. 3151–3166, 2006.

[16] J. P. Thomesse, "Fieldbus Technology in Industrial Automation," *Proceedings of the IEEE*, vol. 93, no. 6, pp. 1073-1101, 2005.

[17] W. C. Chan, *Performance Analysis of Telecommunications and Local Area Networks*, Kluwer International Series in Engineering and Computer Science, 2002.

[18] H. Yang and B. Sikdar,"Performance Analysis of Polling based TDMA MAC Protocols with Sleep and Wakeup Cycles," *in Proc. IEEE International Communications Conference, ICC'07*, pp. 241–246, 2007.

[19] H. Zhang, T. A. Gulliver, "Biorthogonal pulse position modulation for time-hopping multiple access UWB communications," *IEEE Transactions on Wireless Communications*, vol. 4, no. 3, pp. 1154–1162, May 2005.

[20] S. Haykin, *Adaptive Filter Theory; 3rd Edition*, Prentice Hall Information and System Sciences Series, 1996.

[21] A. F. Molisch, K. Balakrishnan, D. Cassioli, C. C. Chong, S. Emami and J. Karedal, "IEEE 802.15.4a Channel Model-final report," *Taskgroup 4a (TG4a),Tech. Report*, 2004.

Farah Haroon received her Masters of Electrical Engineering degree from NED University of Engineering and Technology, Pakistan in 2003. She is currently a PhD student in Telecommunications Field of Study, Asian Institute of Technology, Thailand. Her research interests are ultra wide band communications, propagation and reception in multipath channel and industrial wireless networks.

Kazi Mohiuddin Ahmed received his M.Sc. Engg degree in Electrical Engineering from the Institute of Communications, Leningrad, USSR, and the PhD degree from the University of Newcastle, NSW, Australia, in 1978 and 1983, respectively. Currently, he is a Professor of telecommunications in Asian Institute of Technology, Thailand. His current research interests are in wireless communications and communication networks. Mr. Ahmed is a member of IEEE, IEICE and life member of Bangladesh Electronic Society (BES).